



# Comparative study of hybrid (graphene/magnesium oxide) and ternary hybrid (graphene/zirconium oxide/magnesium oxide) nanomaterials over a moving plate

D.G. Prakasha<sup>a</sup>, M.V.V.N.L. Sudharani<sup>b</sup>, K. Ganesh Kumar<sup>a,\*</sup>, Ali J. Chamkha<sup>c</sup>

<sup>a</sup> Department of Mathematics, Davangere University, Davangere, Karnataka, India

<sup>b</sup> Department of Mathematics, P.B. Siddhartha College of arts and science, Vijayawada, AP, India

<sup>c</sup> Faculty of Engineering, Kuwait College of Science and Technology, Doha District 35004, Kuwait

## ARTICLE INFO

### Keywords:

Slip flow  
Nonlinear radiation  
Hybrid nanomaterial  
Ternary hybrid nanomaterial  
Heat transfer

## ABSTRACT

In the last few decades, the focus has shifted to hybrid nanomaterial flows because of the growing need for energy and the many ways it can be used. However, there is still a lot to learn about these flows. Viewing this analysis is done to look at the flow to study the incompressible flow and heat transfer toward a moving surface with nonlinear radiation. The scaling similarity transformations are employing to convert nonlinear partial differential equations to the nonlinear ordinary differential equations. Here, after converting equations from dimensional to non-dimensional, we will use the BVP4C solver (MATLAB) for plotting the graphs to analyze how distinct non-dimensional parameters effecting the Skin friction and Nusselt number transfer rate for both hybrid fluid (Graphene + Magnesium oxide) case and ternary hybrid nanomaterial (Graphene+ Zirconium oxide +Magnesium oxide) case. Additionally, ethylene glycol was used as the basis fluid for both the binary and ternary hybrid nanomaterials in this investigation. The major outcomes disclosed that the Nusselt number, which measures the rate at which heat is transferred, is higher in ternary hybrid nanomaterial when compared to hybrid nanomaterial flow. Furthermore, the rate of heat transfer rate of the ternary hybrid nanomaterial improves more than that of the hybrid nanomaterial fluid. And also the velocity of the fluid decreased when the  $\delta$  parameter was increased.

## 1. Introduction

Nano-fluids, also known as nano-particle suspensions in a conventional fluid, are used to improve simultaneous heat transport. Nano-particles have gained more and more attention from scientists in recent decades [1] because to their potential applications in several fields, including biomedicine, food processing, electronics, biomaterials, and mechanical technologies. In addition, the movement of the corresponding nanoparticles in the systems that have been described is highly reliant on specific cancer treatment strategies, regulated drug transfer, nanomaterials, fermentation production, and chemotherapy. The fundamental idea of nano-fluids was created in [2] as a solution to this problem. It is possible for a nanomaterial that is composed of nanoparticles that are composed of one to one hundred of these components (atoms) to enhance heating efficiency and, as a result, speed up the transfer of heat. Nanoparticles are components of the base liquid that are

so very tiny that they have the ability to enhance phenomena [3]. The relevance of nanoparticles may also be recognized in the field of medical sciences, namely in areas such as drug transfer, diagnostic techniques, hyperthermia, artificial lungs, the treatment process, heat diseases, cancer, and other fields of application [4–8].

According to the findings of experimental study, the primary objective of combining two separate particles inside the foundational liquid is to enhance the thermal efficiency of the system. The idea of a hybrid nanomaterial was investigated statistically as well as physically by Suresh et al. [9], who also looked into the subject. According to their results, hybrid nanomaterials enhanced the rate of heat transfer on the surface when compared to both useful nanomaterials and basic heated fluids. This was the conclusion drawn from their research. The researchers were given access to a wide variety of strategies for dealing with the hybrid nanomaterial pasture thanks to this point of view. Baghbanzadeh et al. [10] examined the many spherical hybrid nano-structures that were composed of multiwall silica nanotubes. In addition

\* Corresponding author.

E-mail address: [ganikganesh@gmail.com](mailto:ganikganesh@gmail.com) (K.G. Kumar).

Nomenclature	
$u$ and $v$	velocity components of the nanomaterial along the $x$ and $y$
$\sigma^*$	Stefan–Boltzmann
$k^*$	mean absorption coefficient
$q_r$	radiative heat flux,
$\mu_{hnf}$	viscosity of hybrid nanomaterial
$k_{hnf}$	thermal conductivity of hybrid nanomaterial
$\rho_{hnf}$	density of hybrid nanomaterial
$(\rho C_p)_{hnf}$	Heat capacity of hybrid nanomaterial
$Re$	Local Reynolds number
$\theta_w$	Temperature ratio parameter
$R$	Radiation parameter
$\mu_{thnf}$	viscosity of hybrid nanomaterial
$k_{thnf}$	thermal conductivity of hybrid nanomaterial
$A$	Velocity slip constant
$T_\infty$	Ambient temperature
$T_w$	surface temperature
$\phi_1, \phi_2$ and $\phi_3$	Nanoparticle volume fraction
$T$	Temperature of nanomaterial
$U_\infty$	free stream
$U_w$	constant velocity
$\mu_{thnf}$	viscosity of ternary hybrid nanomaterial
$k_{thnf}$	thermal conductivity of ternary hybrid nanomaterial
$\rho_{thnf}$	density of ternary hybrid nanomaterial
$(\rho C_p)_{thnf}$	Heat capacity of ternary hybrid nanomaterial
$\rho_{hnf}$	density of hybrid nanomaterial
$(\rho C_p)_{hnf}$	Heat capacity of hybrid nanomaterial
$\delta$	slip parameter

to this, he gave some thought to the investigation of the thermal conductivity of the associated nanomaterial. Nine et al. [11] investigate the thermophysical characteristics of  $Al_2O_3 - MWCNT /water$ . Hosseinzadeh et al. [12] discussed the optimization of hybrid nanoparticles with mixture fluid flow in an octagonal porous medium by effect of radiation and magnetic field. Zangoosea et al. [13] investigate the hydrothermal analysis of hybrid nanofluid flow on a vertical plate by considering slip condition. Talebi et al. [14] studied the mixture-based dusty hybrid nanofluid flow in porous media affected by magnetic field using. Recently, numerous researchers have analysed and experimented with hybrid nanomaterials [15–24].

Tri-hybrid nanomaterials are relatively new concepts that demonstrate the simultaneous action of three nanoparticles in a single fluid. More research is being devoted to this recently created tri-hybrid mixture model since it outperforms both the hybrid and nanomaterial variants. Tri-hybrid nanomaterial research is prominent in heat transport issues and has numerous practical implications in other areas of physics. In their discussion of the use of a tri-hybrid nanomaterial based on water for advanced thermal applications in a radiator, Arif et al. [25] emphasised and provided some context for the dispersion of nanoparticles of varying sizes and shapes. A similar novel correlation for tri-hybrid nanomaterials with heat transfer applications was established by Sahoo and Kumar [26]. In order to improve thermal performance, Xuan et al. [27] studied the sensitivity analysis of tri-hybrid nano-liquids. Lately, Ahmad et al. [28] conducted study on heat transmission using tri-hybrid nano-liquids with applications. The fluid containing three nanoparticles was analysed and synthesized by Adun et al. [29] using a combination of  $Fe_3O_4$ ,  $Al_2O_3$ , and  $ZnO$  in a water base fluid; they also determined the influence of  $\phi$ , on the fluid's temperature. Furthermore, a hybrid machine for prediction was constructed in this research. Regenerative evaporative coolers utilising a combination of three nanoparticles were analysed by Kashyap et al. [30], who determined that the cooler's thermal performance and temperature might be improved. Using mathematics, Kumar and Sahoo [31] analysed the effects of three variables on the fluid and its uses in an air heat exchanger.

Slip flow across a linearly stretching sheet was the topic of this essay. An examination of the transfer of heat and flow over a linearly moving sheet is made. In addition, the hybrid nanomaterial, Graphene and Magnesium Oxide are combined, and Ethylene Glycol is used as the working liquid. In the ternary nanomaterial, Graphene, Zirconium Oxide and Magnesium Oxide are all combined, and Ethylene Glycol is used as the working liquid. The governing equations (equation of motion and energy equation) are transformed into a system of nonlinear ODE's that can be solved numerically in MATLAB by applying the appropriate similarity transformations. The impacts of the controlling parameters are illustrated graphically here in terms of the velocities and temperature profiles. Analyses of the similarities and differences between

hybrid nanomaterial and ternary hybrid nanomaterial are investigated. To have a check on the accuracy of the numerical procedure used, first test computations for  $\theta'(0)$  are carried out for different values of  $Pr$  and then they are compared with the available published results of Mania Goyal and Bhargava [33], and Gorla and Sidawi [32] in Table-2 and they are found to be in excellent agreement

### 1.1. Mathematical formulation

Consider a steady flow and heat transfer of hybrid and Tri hybrid nanomaterial over a moving frame. The plate is same or opposite direction to the free stream  $U_\infty$  and constant velocity  $U_w$ . The flow is confined to  $y > 0$  and sheet coincides with the plane  $y = 0$ . The ambient fluid temperature is a constant  $T_\infty$ . Furthermore, it is pretended that the Rosseland approximation. In addition, the hybrid nanomaterial, Graphene and Magnesium Oxide are combined, and Ethylene Glycol is used as the working liquid. In the ternary nanomaterial, Graphene, Zirconium Oxide and Magnesium Oxide are all combined, and Ethylene Glycol is used as the working liquid.

Governing equations of hybrid nanomaterial are defined below [34];

$$\frac{\partial u}{\partial x} + \frac{\partial v}{\partial y} = 0, \tag{1}$$

$$u \frac{\partial u}{\partial x} + v \frac{\partial u}{\partial y} = \frac{\mu_{hnf}}{\rho_{hnf}} \frac{\partial^2 u}{\partial y^2} \tag{2}$$

$$(\rho C_p)_{hnf} \left[ u \frac{\partial T}{\partial x} + v \frac{\partial T}{\partial y} \right] = \frac{\partial}{\partial y} \left[ \left( k_{hnf} + \frac{16\sigma^* T^3}{3k^*} \right) \frac{\partial T}{\partial y} \right] + \left( \frac{\partial u}{\partial y} \right)^2 \tag{3}$$

Governing equations of ternary hybrid nanomaterial are defined below [35,36];

$$\frac{\partial u}{\partial x} + \frac{\partial v}{\partial y} = 0, \tag{4}$$

$$u \frac{\partial u}{\partial x} + v \frac{\partial u}{\partial y} = \frac{\mu_{thnf}}{\rho_{thnf}} \frac{\partial^2 u}{\partial y^2} \tag{5}$$

$$(\rho C_p)_{thnf} \left[ u \frac{\partial T}{\partial x} + v \frac{\partial T}{\partial y} \right] = \frac{\partial}{\partial y} \left[ \left( k_{thnf} + \frac{16\sigma^* T^3}{3k^*} \right) \frac{\partial T}{\partial y} \right] + \left( \frac{\partial u}{\partial y} \right)^2. \tag{6}$$

where  $u$  and  $v$  denotes the velocity components of the nanomaterial along the  $x$  and  $y$  directions commonly,  $\sigma^*$ - Stefan–Boltzmann constant and  $k^*$ - mean absorption coefficient,  $q_r$  - radiative heat flux,

The thermophysical properties  $\mu_{hnf}$ ,  $k_{hnf}$ ,  $(\rho C_p)_{hnf}$  and  $\rho_{hnf}$  for hybrid nanomaterial (Graphene +Magnesium oxide) are defined as;

The hybrid nanomaterial density model by:

$$\frac{\rho_{hnf}}{\rho_f} = (1 - \phi_2) [(1 - \phi_1)\rho_f + \phi_1\rho_{s1}] + \phi_2\rho_{s2}$$

The hybrid nanomaterial specific heat model by:

$$(\rho C_p)_{hnf} = (1 - \phi_2) [(1 - \phi_1)(\rho C_p)_f + \phi_1(\rho C_p)_{s1}] + \phi_2(\rho C_p)_{s2}$$

The hybrid nanomaterial viscosity model by:

$$\frac{\mu_{hnf}}{\mu_f} = \frac{1}{(1 - \phi_1)^{2.5} (1 - \phi_2)^{2.5}}$$

The hybrid nanomaterial thermal conduction model by;

$$\frac{k_{hnf}}{k_{bf}} = \frac{k_2 + 2k_{bnf} - 2\phi_2(k_{bnf} - k_2)}{k_2 + 2k_{bnf} + \phi_2(k_{bnf} - k_2)}$$

where

$$\frac{k_{bf}}{k_f} = \frac{k_1 + 2k_f - 2\phi_1(k_f - k_1)}{k_1 + 2k_f + \phi_1(k_f - k_1)}$$

The expression for  $\mu_{hnf}(\beta)$ ,  $k_{hnf}$ ,  $(\rho C_p)_{hnf}$  and  $\rho_{hnf}$  of the ternary hybrid nanomaterial (Graphene+ Zirconium oxide +Magnesium oxide) is as follows;

The ternary hybrid nanomaterial viscosity model by:

$$\frac{\mu_{thnf}}{\mu_f} = \frac{1}{(1 - \phi_1)^{2.5} (1 - \phi_2)^{2.5} (1 - \phi_3)^{2.5}}$$

The ternary hybrid nanomaterial density model by:

$$\frac{\rho_{thnf}}{\rho_f} = (1 - \phi_1) \left\{ (1 - \phi_2) \left[ (1 - \phi_3) + \frac{\phi_3(\rho C_p)_{s3}}{\rho_f} \right] + \frac{\phi_2(\rho C_p)_{s2}}{\rho_f} \right\} + \frac{\phi_1(\rho C_p)_{s1}}{\rho_f}$$

The ternary hybrid nanomaterial specific heat model by:

$$\frac{\rho_{thnf}}{(\rho C_p)_f} = \frac{\phi_1(\rho C_p)_{s1}}{\rho_f} + (1 - \phi_1) \left\{ (1 - \phi_2) \left[ (1 - \phi_3) + \frac{\phi_3(\rho C_p)_{s3}}{\rho_f} \right] + \frac{\phi_2(\rho C_p)_{s2}}{\rho_f} \right\}$$

The ternary hybrid nanomaterial thermal conduction model by;

$$\frac{k_{thnf}}{k_{hnf}} = \frac{k_3 + 2k_{hnf} - 2\phi_3(k_{hnf} - k_3)}{k_3 + 2k_{hnf} + \phi_3(k_{hnf} - k_3)}, \quad \frac{k_{hnf}}{k_{bf}} = \frac{k_2 + 2k_{bnf} - 2\phi_2(k_{bnf} - k_2)}{k_2 + 2k_{bnf} + \phi_2(k_{bnf} - k_2)}$$

$$\frac{k_{bf}}{k_f} = \frac{k_1 + 2k_f - 2\phi_1(k_f - k_1)}{k_1 + 2k_f + \phi_1(k_f - k_1)}$$

Interrelated boundary conditions are accustomed by;

$$u = U_w + A\nu_f \frac{\partial u}{\partial y}, v = 0, T = T_w \text{ at } y = 0,$$

$$u \rightarrow 0, T \rightarrow T_\infty \text{ as } y \rightarrow \infty \tag{7}$$

Now introduce the similarity transformation as;

$$u = Uf'(\eta), v = \sqrt{\frac{\nu_f U}{2x}}(\eta f'(\eta) - f(\eta)), T = T_w(1 + (\theta_w - 1)\theta(\eta)), \eta = \sqrt{\frac{U}{2\nu_f x}}y \tag{8}$$

where  $U = U_w + U_\infty$ ,  $\theta_w = \frac{T_w - T_\infty}{T_w}$ ,  $\theta_w > 1$ .

Making use of Eq. (5), Eq. (1) is identically satisfied and Eqs. (2) and (3) takes the form,

For hybrid nanomaterial case

$$\frac{\mu_{hnf} f'''}{\mu_f} + \frac{\rho_{hnf} f f'''}{\rho_f} - f'2 = 0 \tag{9}$$

$$\frac{k_{hnf}}{k_f} R [(1 + (\theta_w - 1)\theta)^3 \theta' + 3(\theta_w - 1)\theta'^2 (1 + (\theta_w - 1)\theta)^2] +$$

$$Pr \left[ (1 - \phi_2) \left[ (1 - \phi_1) + \phi_1 \left( \frac{(\rho C_p)_{s1}}{(\rho C_p)_f} \right) \right] + \phi_2 \left( \frac{(\rho C_p)_{s2}}{(\rho C_p)_f} \right) \right] (f\theta' + Ec f'^2) = 0 \tag{10}$$

For ternary hybrid nanomaterial case

$$\frac{\mu_{thnf} f'''}{\mu_f} + \frac{\rho_{thnf} f f'''}{\rho_f} - f'2 = 0 \tag{11}$$

$$\frac{k_{thnf}}{k_f} R [(1 + (\theta_w - 1)\theta)^3 \theta' + 3(\theta_w - 1)\theta'^2 (1 + (\theta_w - 1)\theta)^2] +$$

$$Pr \left[ \frac{\phi_1(\rho C_p)_{s1}}{\rho_f} + (1 - \phi_1) \left\{ (1 - \phi_2) \left[ (1 - \phi_3) + \frac{\phi_3(\rho C_p)_{s3}}{\rho_f} \right] + \frac{\phi_2(\rho C_p)_{s2}}{\rho_f} \right\} \right] (f\theta' + Ec f'^2) = 0 \tag{12}$$

Interrelated conditions are in the form;

$$f(0) = 0, f'(0) = 1 + \frac{\delta}{(1 + \phi)^{2.5}} f''(0), \theta(0) = 1, f'(\infty) = 0, \theta(\infty) = 0, \tag{13}$$

where,  $\delta = A \frac{U_w}{\nu_f}$ ,  $Pr = \frac{(\mu c_p)_f}{k_f}$ ,  $Ec = \frac{U_w^2}{(T_w - T_\infty) c_{pf}}$ ,  $R = \frac{16\sigma^* T_w^3}{3k_{nf} k^*}$ .

### 1.2. Engineering quantities of interest

The  $C_{fx}$  and local  $Nu_x$  are prescribe by,

$$\sqrt{Re_x} C_{fx} = \frac{\mu_{thnf} f''(0)}{\mu_f}, \quad \frac{Nu_x}{\sqrt{Re_x}} = -\frac{k_{thnf}}{k_f} (1 + R\theta_w^3) \theta'(0),$$

where  $Re = \frac{U_x}{\nu_f}$  is local Reynolds number.

### 1.3. Numerical method

A numerical method With the assistance of boundary limitations, the non-linear system of ODEs that is being solved with RKF-45 using MATLAB (see Eqs. (9)–(12)) may be solved using the method that is given in (13). This section presents a graphical analysis of the physical influence that a number of different body forces and control factors have on a velocity and temperature profile. There is a tabular representation of the computational values of  $Sh_x(Re)^{-1/2}$  and  $Nu_x Re_x^{-1/2}$ . When the following conditions are  $=6$ ,  $R = 0.6$ ,  $Ec = 0.5$ ,  $\theta_w = 1.2$ , and  $A = 0.5$ . Graphical and numerical results for the relevant variables are produced. The resultant equations are higher order ODE's. In the beginning, we simplify these higher order ODE's into the first order form,

For hybrid nanomaterial case:

$$y_4 = \frac{\mu_f}{\mu_{hnf}} \left[ y_2^2 - \frac{\rho_{hnf}}{\rho_f} y_1 y_3 \right] \tag{14}$$

$$y_7 = -\frac{k_f}{k_{hnf} R [(1 + (\theta_w - 1)y_5)^3]} \left[ \frac{k_{hnf}}{k_f} 3R [(\theta_w - 1)y_6^2 (1 + (\theta_w - 1)y_5)^2] + \right.$$

$$\left. Pr \left[ (1 - \phi_2) \left[ (1 - \phi_1) + \phi_1 \left( \frac{(\rho C_p)_{s1}}{(\rho C_p)_f} \right) \right] + \phi_2 \left( \frac{(\rho C_p)_{s2}}{(\rho C_p)_f} \right) \right] (y_1 y_6 + Ec y_3^2) \right] \tag{15}$$

For ternary hybrid nanomaterial case:

$$y_4 = \frac{\mu_f}{\mu_{thnf}} \left[ y_2^2 - \frac{\rho_{thnf}}{\rho_f} y_1 y_3 \right] \tag{16}$$

$$y_7 = -\frac{k_f}{k_{thnf} R [(1 + (\theta_w - 1) y_5)^3]} \left[ \frac{k_{thnf}}{k_f} 3R [(\theta_w - 1) y_6^2 (1 + (\theta_w - 1) y_5)^2] + \right.$$

$$\left. Pr \left[ \frac{\phi_1 (\rho C p)_{s1}}{\rho_f} + (1 - \phi_1) \left\{ (1 - \phi_2) \left[ \frac{(1 - \phi_3)}{\rho_f} + \frac{\phi_3 (\rho C p)_{s3}}{\rho_f} \right] + \frac{\phi_2 (\rho C p)_{s2}}{\rho_f} \right\} \right] (y_1 y_6 + Ec y_3^2) \right] \tag{17}$$

Interrelated conditions are in the form;

$$y_1(0) = 0, y_2(0) = 1 + \frac{\delta}{(1 + \phi)^{2.5}} y_3(0), y_5(0) = 1, y_2(\infty) = 0, y_5(\infty) = 0, \tag{18}$$

**2. Result and discussion**

In this part, the results of the modulating velocity and heat distributions for various parameters are shown visually as an output to highlight the underlying physical significance of the data. In addition, exemplary results for the  $Nu_x Re_x^{-1/2}$  and  $C_{fx} Re_x^{-1/2}$  have been documented via graphs for a variety of parameter values for both hybrid and ternary hybrid nanomaterial. Table-1 mentions the Thermophysical properties of hybrid and ternary hybrid nanoparticles. There is a tabular representation of the computational values of  $Nu_x Re_x^{-1/2}$  and  $C_{fx} Re_x^{-1/2}$ , when the following conditions are  $\phi_1 = \phi_2 = \phi_3 = 0.02, \delta = 0.4, Pr = 6, R = 0.5, Ec = 0.5$  and  $\theta_w = 1.3$ . To have a check on the accuracy of the numerical procedure used, first test computations for  $\theta'(0)$  are carried out for viscous fluid for different values of  $Pr$  and then they are compared with the available published results of Mania Goyal and Bhargava [33] and Gorla and Sidawi [32] in Table-2 and they are found to be in excellent agreement.

The stream line consequence of the parameter  $A$  is studied in Figs. 1 (a-b) and 2(a-b) for both hybrid and ternary hybrid nanomaterial, respectively. It can be shown in Fig. 1(a-b) that the augmentation of heat transmission is greater (where  $A = 0.5$ ) in the ternary nanomaterial scenario when compared with the hybrid nanomaterial situation. Fig. 2 (a-b) demonstrates that for the value of  $A(=1)$ , the greater fluid temperature is shown. This can be noticed by comparing the two figures. In addition, the performance of the fluid temperature is greater in the case

of the ternary hybrid fluid than in the case of the hybrid nanomaterial. (See Tables 1 and 2.)

Fig. 3 displays how the friction factor working to varying  $\delta$  versus  $Pr$  parameter values. The friction factor enhances for higher estimates of  $\delta$  versus  $Pr$  parameter. Additionally, friction of the fluid enhances for rising values of  $\delta$  versus  $Pr$ . Furthermore, performance of fluid velocity is more comfortable in ternary hybrid case when treated with hybrid nanomaterial case. Fig. 4 depicts how the  $Pr$  and  $Ec$  parameters influence the  $Nu_x Re_x^{-1/2}$ . This graphic shows that the  $Nu_x Re_x^{-1/2}$  increases with increasing  $Pr$  and  $Ec (<1)$ . However, with larger values of  $Ec (>1)$ , the reverse trend is found. Characteristics of major parameters  $Pr$  and  $R$  on the  $Nu_x Re_x^{-1/2}$  curve exhibit variance in Fig. 5, as  $Nu_x Re_x^{-1/2}$  drops with rising  $Pr$  parameter but reverses with larger  $R$  parameter values.

On Fig. 6, you can see the effect of  $R$  on the  $\theta(\eta)$  profiles of interest for both hybrid and ternary hybrid nanomaterial situation. It indicates that the greater  $R$  value, the more intense the heat provided to the liquid, resulting in an enhancement in thermal layer thickness for both hybrid and ternary hybrid nanomaterial situation. With a higher  $R$ , the heat distribution expands and the environment becomes more of a factor. Furthermore, higher  $R$  values result in a substantial amount of heat being transferred to the fluids.

The impact that  $Ec$  had on the  $\theta(\eta)$  profile for both hybrid and ternary hybrid nanomaterial situation is seen in Fig. 7. It is clear that the  $\theta(\eta)$  field for both hybrid and ternary hybrid nanomaterial situation should be increased in order to raise the  $Ec$  parameter. In addition, there is a correlation between the thickness of the layer and a thicker behaviour for increasing  $Ec$  values. From a physical standpoint, both electrical energy and mechanical energy convert into heat through internal friction of the fluid. Thus, the thermal layer thickness and temperature distribution will both increase with an increase in  $Ec$ . Fig. 8 explores the characteristics of  $\theta(\eta)$  for both hybrid and ternary hybrid nanomaterial situation versus rising values of  $\theta_w$ . One can observe from this figure that  $\theta(\eta)$  and layer thickness for both hybrid and ternary hybrid nanomaterial situation booms for larger  $\theta_w$ . Furthermore, enhancement of fluid temperature is also enriched all there fluid case for riding values of  $\theta_w$ . In addition, the enchantment of fluid temperature is most prominent in the instance when ternary hybrid nanomaterial case, followed by the hybrid nanomaterial case.

For both hybrid and ternary hybrid nanomaterial situation, the impact of the Prandtl number  $Pr$  versus the thermal profile ( $\theta(\eta)$ ) is shown in Fig. 9. For both the hybrid and ternary hybrid nanomaterial instance, the temperature of the liquid lowers dramatically as the  $Pr$  increases. This is because when  $Pr$  increases, the liquid's thermal diffusivity reduces, and the temperature drops. In addition, ternary hybrid nanomaterials provide a greater fluid temperature advantage than

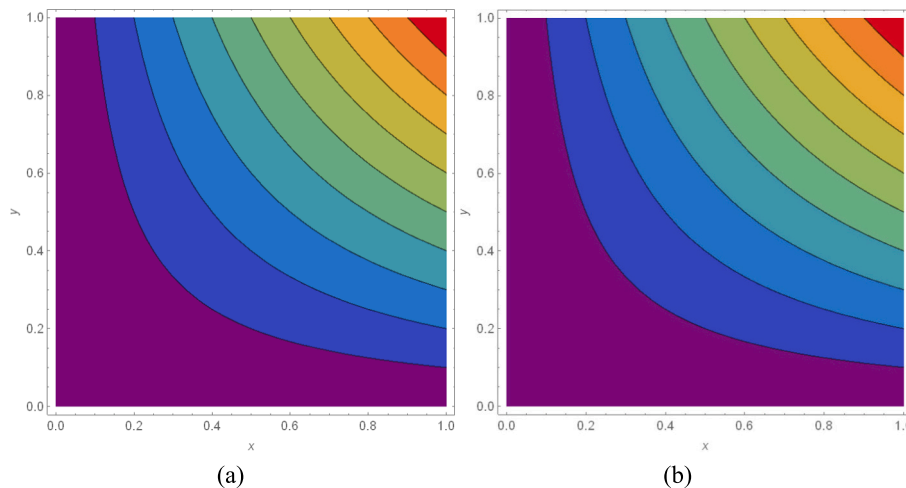


Fig. 1. a) Stream lines for hybrid nanofluid A = 0.5, b) Stream lines for ternary hybrid nanofluid A = 0.5.

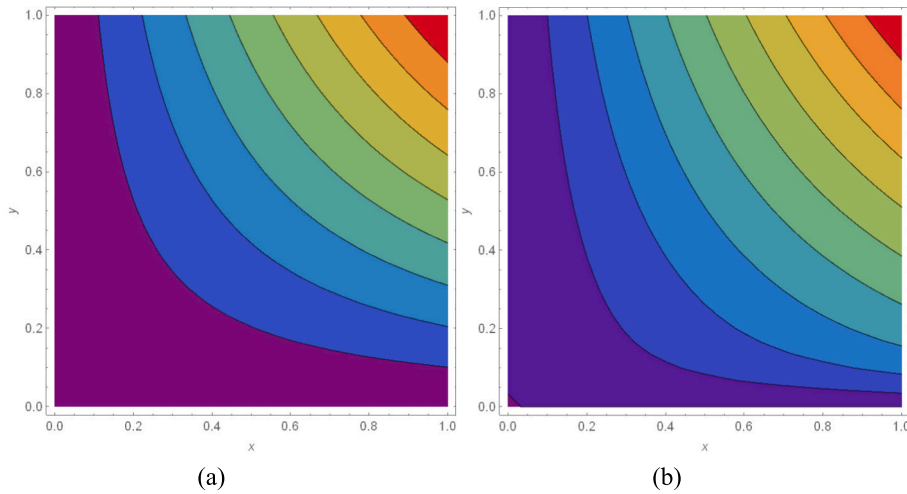


Fig. 2. a) Stream lines of hybrid nanofluid for  $A = 1$ . b). Stream lines of ternary hybrid nanofluid for  $A = 1$ .

Table 1

Thermophysical properties of a Hybrid (Graphene+Magnesium oxide) and Ternary hybrid nanomaterial (Graphene+Zirconium oxide+Magnesium oxide) [8,7,16,21,35].

Thermophysical property	fluid base	Hybrid nanomaterial		Ternary hybrid nanomaterial		
	EG	Graphene	Magnesium oxide	Graphene	Zirconium oxide	Magnesium oxide
$\rho$ (kg/m <sup>3</sup> )	1114.0	2200	3560	2200	5680	3560
$\rho C_p$ (j/kgK)	2415	5000	955	5000	502	955
$k$ (w/mk)	0.2520	790	45	790	1.7	45

Table 2

Comparison table for  $-\theta'(0) Ec = R = \phi_1 = \phi_2 = \phi_3 = Ec = 0$ .

Pr	Govil and Sidawi [32]	M. Goyal and Bhargava [33]	Present
0.2	0.1691	0.1691	0.170259788
0.7	0.5349	0.4539	0.454447258
2	0.9114	0.9113	0.911352755
7	1.8905	1.8954	1.895400395

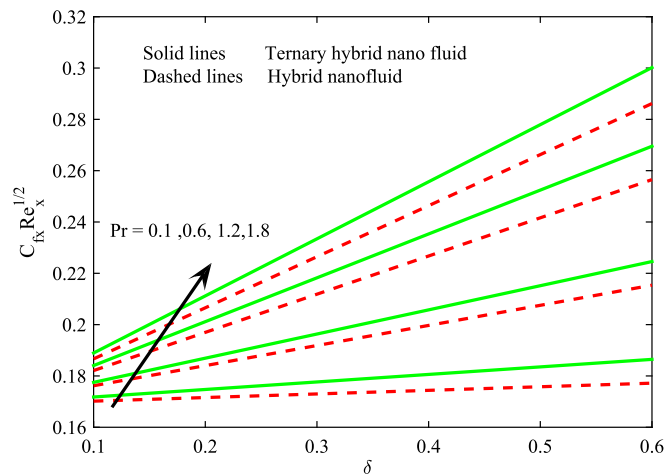


Fig. 3. Effect of  $\delta$  versus Pr on  $C_{fx}$

hybrid nanomaterials. For the hybrid and ternary hybrid nanomaterial examples, the impact of  $\phi_1$ ,  $\phi_2$  and  $\phi_3$  on the  $f'(\eta)$  profile is shown in Figs. 10–12. In both the hybrid and the ternary hybrid nanomaterial case, the velocity curve accelerates as a result of the addition of solid nanoparticles to the nanomaterial. Collisions between widely scattered

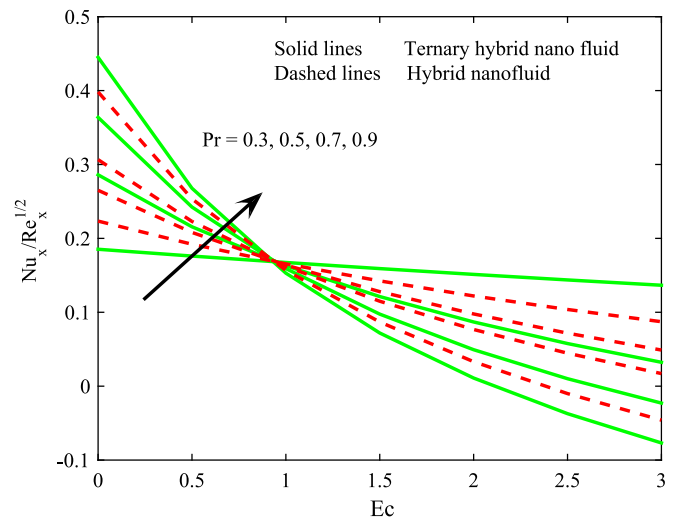


Fig. 4. Effect of  $Ec$  versus Pr on  $Nu_x$

nanoparticles are responsible for this result. In addition, for both nanomaterial situations shown in Figs. 10 and 12, it is important to notice that the values of  $\phi_1$ ,  $\phi_2$  and  $\phi_3$  have increased in order to enhance the appropriate layer thickness.

Figs. 13–15 highlights the effect of the  $\phi_1$ ,  $\phi_2$  and  $\phi_3$  parameters on the temperature profile of the hybrid and ternary hybrid nanomaterial instance, respectively. When the nanoparticle releases its stored energy, it does so in the form of heat. Therefore, in both the binary and ternary hybrid nanomaterial examples, the mixing of extra nanoparticles may need more energy, increasing the breadth of the temperature and boundary layer. Additionally, fluid temperature may be better regulated in ternary hybrid nanomaterial situations than in hybrid nanomaterial cases. The impact that  $\delta$  had on the  $f'(\eta)$  profile for both hybrid and

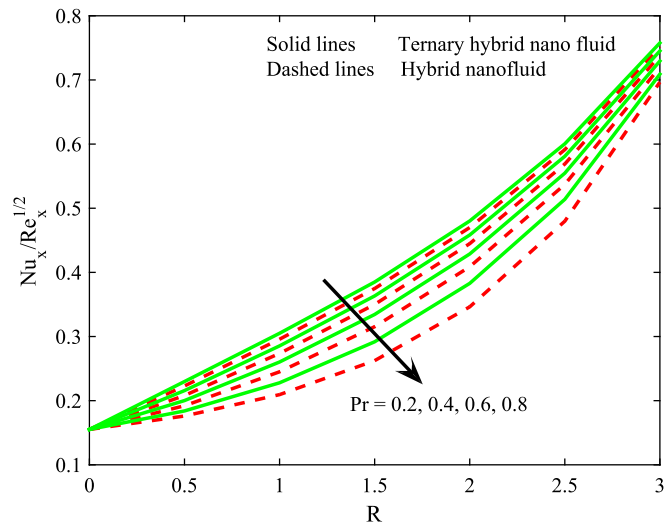


Fig. 5. Effect of R versus Pr on  $Nu_x$

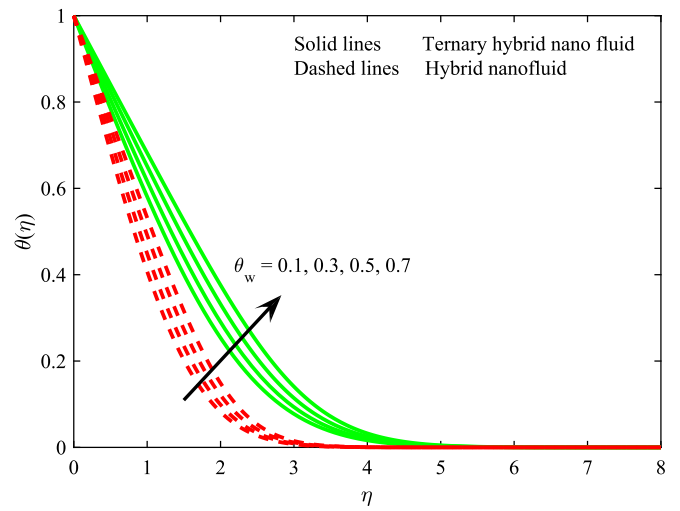


Fig. 8. Effect of  $\theta_w$  on  $\theta(\eta)$

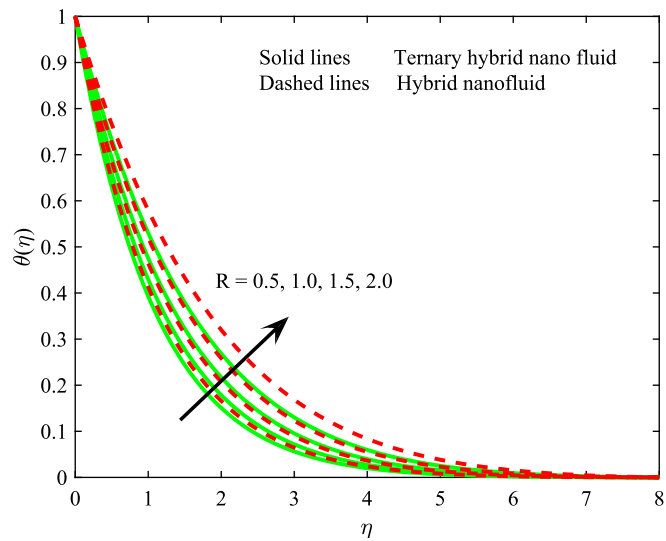


Fig. 6. Effect of R on  $\theta(\eta)$

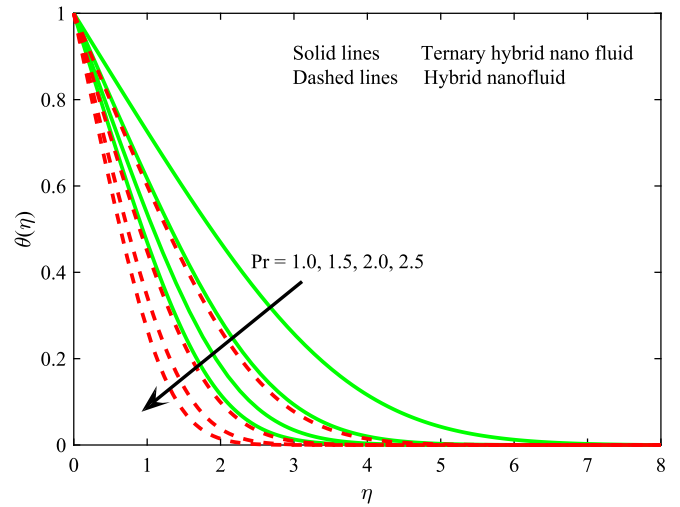


Fig. 9. Effect of Pr on  $\theta(\eta)$

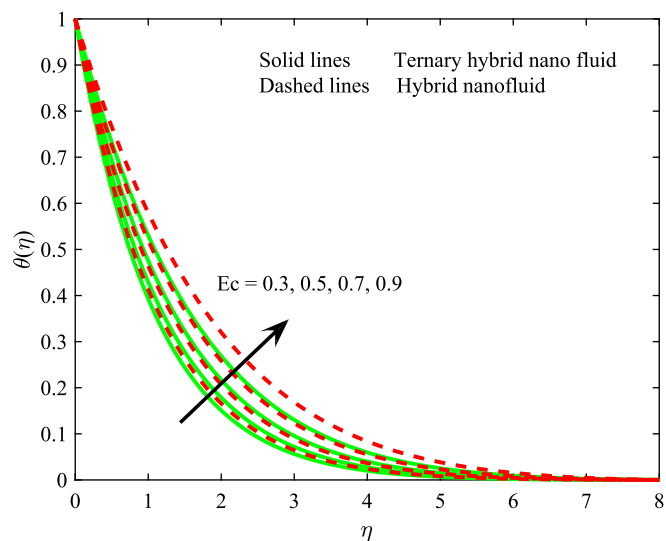


Fig. 7. Effect of Ec on  $\theta(\eta)$

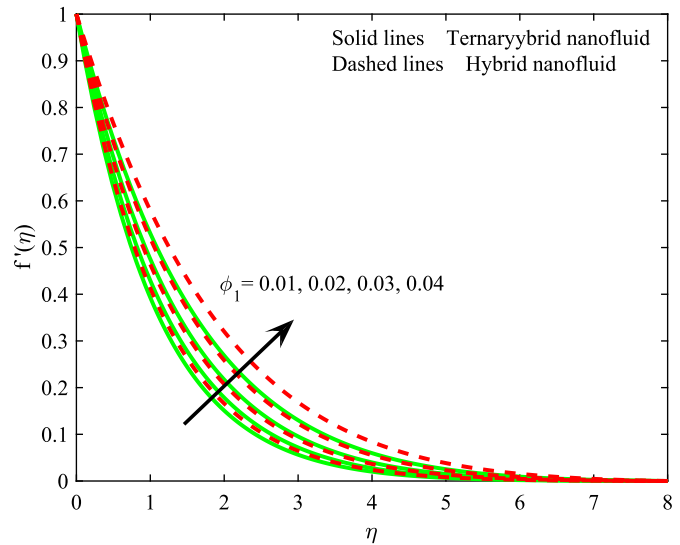


Fig. 10. Effect of Ec on  $\theta(\eta)$

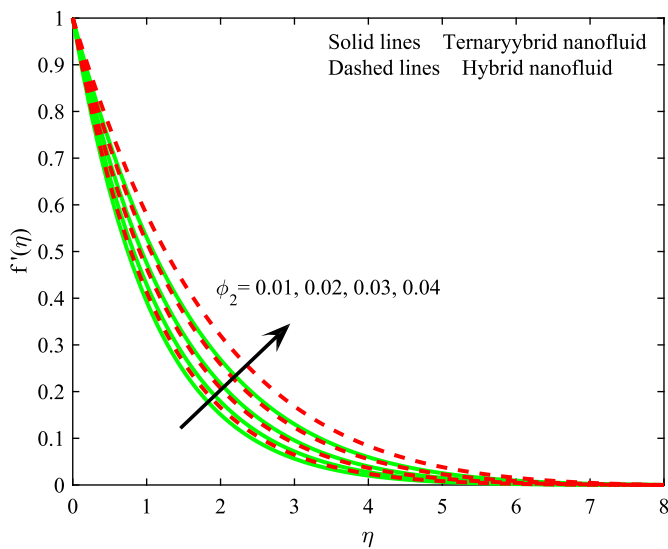


Fig. 11. Effect of  $\phi_2$  on  $f'(\eta)$

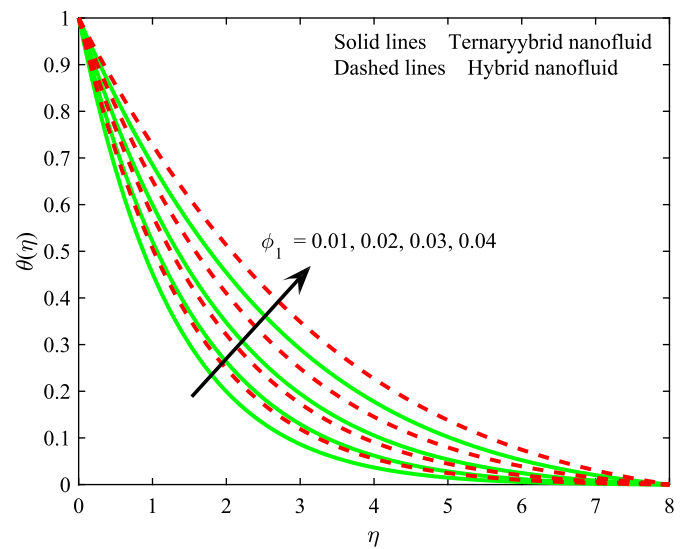


Fig. 13. Effect of  $\phi_1$  on  $\theta(\eta)$

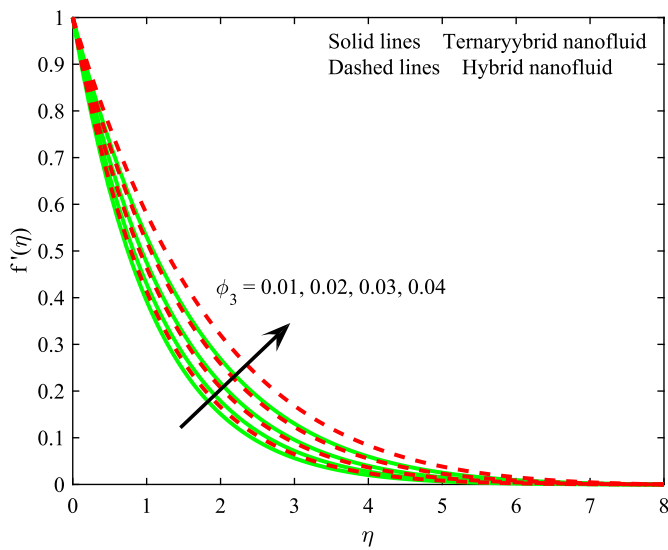


Fig. 12. Effect of  $\phi_3$  on  $f'(\eta)$

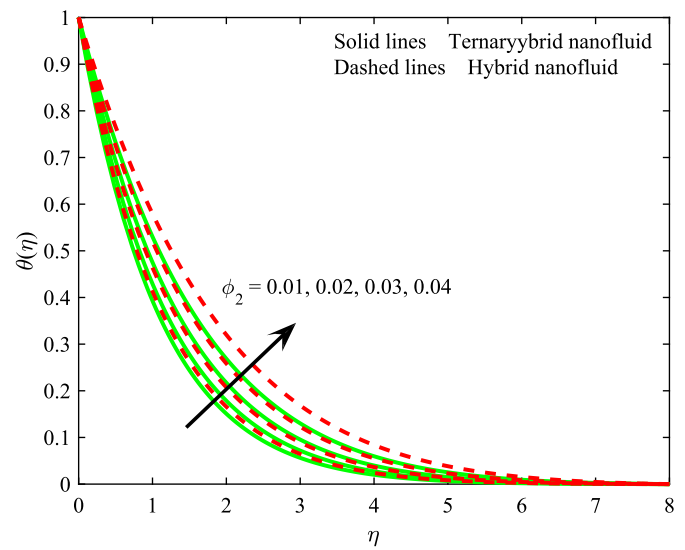


Fig. 14. Effect of  $\phi_2$  on  $\theta(\eta)$

ternary hybrid nanomaterial situation is seen in Fig. 16. It is clear that the  $f'(\eta)$  field for both hybrid and ternary hybrid nanomaterial situation should be decreased in order to raise the  $\delta$  parameter.

2.1. Final remarks

In this paper, hybrid nanomaterial, ternary hybrid nanomaterial model, and slip effects are demonstrated, taking into consideration the flow and radiative heat transfer across a stretched surface. Both numerical and graphical analysis is used to expound on the impact that the physical parameters have. The most important findings may be summarized as follows:

- The heat transfer rate of the ternary hybrid nanomaterial improves more than that of the hybrid nanomaterial fluid.
- An increasing the parameters  $\phi_1$ ,  $\phi_2$  and  $\phi_3$  improves the velocity profile.
- Higher  $Pr$  values invalidate the existence of a thermal layer.
- The velocity of the fluid decreased when the  $\delta$  parameter was increased.

The temperature of the fluid improves the values of  $Ec, R$  and  $\theta_w$ . Temperature profile rises for booming values of  $\phi_1$ ,  $\phi_2$  and  $\phi_3$  parameter.

Availability of data and material

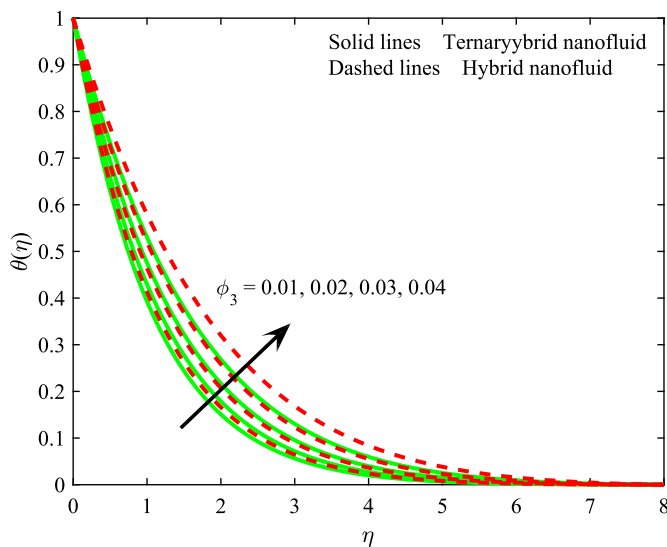
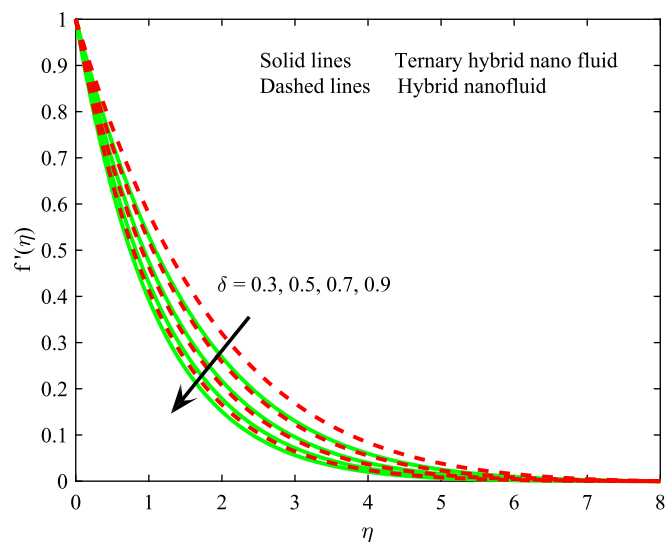
All data that support the findings of this study are included within the article (and any supplementary files).

Credit author statement

- D.G. Prakasha: Formulation of the problem.
- M.V.V.N.L. Sudharani: Calculation of the problem.
- K. Ganesh Kumar: literature review and survey.
- Ali J. Chamkha: written the manuscript.

Declaration of Competing Interest

The authors declare that there is no conflict of interest.

Fig. 15. Effect of  $\phi_3$  on  $\theta(\eta)$ Fig. 16. Effect of  $\delta$  on  $\theta(\eta)$ 

### Data availability

No data was used for the research described in the article.

### Acknowledgment

The author thanks the University Grants Commission's Dr. D. S. Kothari Post-Doctoral Fellowship Program for Funding.

### References

- H. Waqas, U. Farooq, M.S. Alqarni, T. Muhammad, Numerical investigation for 3D bioconvection flow of Carreau nanomaterial with heat source/sink and motile microorganisms, *Alexandr. Eng. J.* 61 (3) (2022) 2366–2375.
- D. Habib, N. Salamat, S. Abdal, I. Siddique, M.C. Ang, A. Ahmadian, On the role of bioconvection and activation energy for time dependent nanomaterial slip transpiration due to extending domain in the presence of electric and magnetic fields, *Ain Shams Eng. J.* 13 (1) (2022), 101519.
- M.T. Sk, K. Das, P.K. Kundu, Multiple slip effects on bioconvection of nanomaterial flow containing gyrotactic microorganisms and nanoparticles, *J. Mol. Liquids* 220 (2016) 518–526.
- K. Ganesh Kumar, B.J. Gireesha, S. Manjunatha, N.G. Rudraswamy, Effect of nonlinear thermal radiation on double-diffusive mixed convection boundary layer flow of viscoelastic nanofluid over a stretching sheet, *Int. J. Mech. Mat. Eng.* 12 (1) (2017) 1–18.
- O.D. Makinde, K.G. Kumar, S. Manjunatha, B.J. Gireesha, Effect of nonlinear thermal radiation on MHD boundary layer flow and melting heat transfer of micropolar fluid over a stretching surface with fluid particles suspension, *Defect Diffus. Forum* 378 (2017) 125–136.
- K.G. Kumar, B.J. Gireesha, N.G. Rudraswamy, S. Manjunatha, Radiative heat transfers of Carreau fluid flow over a stretching sheet with fluid particle suspension and temperature jump, *Res. Phys.* 7 (2017) 3976–3983.
- M.G. Reddy, K.G. Kumar, Cattaneo-Christov heat flux feature on carbon nanotubes filled with micropolar liquid over a melting surface: a stream line study, *Int. Commun. Heat Mass Transf.* 122 (2021), 105142.
- K.G. Kumar, A.J. Chamkha, Darcy-Forchheimer flow and heat transfer of water-based Cu nanoparticles in convergent/divergent channel subjected to particle shape effect, *Eur. Phys. J. Plus* 134 (3) (2018) 107.
- S. Suresh, K.P. Venkataraj, P. Selvakumar, M. Chandrasekar, Effect of Al<sub>2</sub>O<sub>3</sub>-Cu/water hybrid nanomaterial in heat transfer, *Exp. Thermal Fluid Sci.* 38 (2012) 54–60.
- M. Baghbanzadeh, A. Rashidi, D. Rashtchian, R. Lotfi, A. Amrollahi, Synthesis of spherical silica/multiwall carbon nanotubes hybrid nanostructures and investigation of thermal conductivity of related nanomaterials, *Thermochimica Acta* 549 (2012) 87–94.
- M.J. Nine, M. Batmunkh, J.H. Kim, H.S. Chung, H.M. Jeong, Investigation of Al<sub>2</sub>O<sub>3</sub>-MWCNTs hybrid dispersion in water and their thermal characterization, *J. Nanosci. Nanotechnol.* 12 (6) (2012) 4553–4559.
- Kh. Hosseinzadeh, So Roghani, A.R. Mogharrebi, A. Asadi, D.D. Ganji, Optimization of hybrid nanoparticles with mixture fluid flow in an octagonal porous medium by effect of radiation and magnetic field, *J. Therm. Anal. Calorim.* 143 (2) (2021) 1413–1424.
- M.R. Zangooee, Kh. Hosseinzadeh, D.D. Ganji, Hydrothermal analysis of hybrid nanofluid flow on a vertical plate by considering slip condition, *Theor. Appl. Mech. Lett.* 12 (5) (2022) 100357.
- R.H. Talebi, Fallah Najafabadi, M.M. Hosseinzadeh Kh, D.D. Ganji, Investigation of mixture-based dusty hybrid nanofluid flow in porous media affected by magnetic field using, *Int. J. Ambient Energy* 43 (1) (2022) 6425–6435.
- Kh. Hosseinzadeh, Moloud Mardani, M. Salehi, D.D. Paikar Ganji, Investigation of micropolar hybrid nanofluid (iron oxide–molybdenum disulfide) flow across a sinusoidal cylinder in presence of magnetic field, *Int. J. Appl. Comp. Math.* (2021), <https://doi.org/10.1007/s40819-021-01148-6>.
- Kh. Hosseinzadeh, M.R. Mardani, M. Paikar, M. Waqas, D.D. Ganji, Entropy generation of three-dimensional Bödewadt flow of water and hexanol base fluid suspended by Fe<sub>3</sub>O<sub>4</sub> and MoS<sub>2</sub> hybrid nanoparticles, *Pramana* 95 (2) (2021).
- K. Hosseinzadeh, A. Asadi, A.R. Mogharrebi, D.D. Ganji, Investigation of mixture fluid suspended by hybrid nanoparticles over vertical cylinder by considering shape factor effect, *J. Therm. Anal. Calorim.* 143 (2021) 1081–1095.
- M.R. Zangooee, Kh. Hosseinzadeh, D.D. Ganji, Investigation of three-dimensional hybrid nanofluid flow affected by nonuniform MHD over exponential stretching/shrinking plate, *Nonlin. Eng.* (2022), <https://doi.org/10.1515/nleng-2022-0019>.
- K. Hosseinzadeh, E. Montazer, M.B. Shafii, D.D. Ganji, Heat transfer hybrid nanofluid (1-Butanol/MoS<sub>2</sub>-Fe<sub>3</sub>O<sub>4</sub>) through a wavy porous cavity and its optimization, *Int. J. Numer. Methods Heat Fluid Flow* 31 (5) (2021) 1547–1567.
- K. Muhammad, T. Hayat, A. Alsaedi, B. Ahmed, A comparative study for convective flow of basefluid (gasoline oil), nanomaterial (SWCNTs) and hybrid nanomaterial (SWCNTs + MWCNTs), *Appl. Nanosci.* 11 (2021) 9–20.
- K. Muhammad, T. Hayat, A. Alsaedi, Numerical study of Newtonian heating in flow of hybrid nanofluid (SWCNTs + CuO + ethylene glycol) past a curved surface with viscous dissipation, *J. Therm. Anal. Calorim.* 143 (2021) 1291–1302.
- K. Muhammad, T. Hayat, A. Alsaedi, S. Momani, Mixed convective slip flow of hybrid nanofluid (MWCNTs + Cu + water), nanofluid (MWCNTs + Water) and base fluid (water): a comparative investigation, *J. Therm. Anal. Calorim.* 143 (2021) 1523–1536.
- K. Muhammad, T. Hayat, A. Alsaedi, B. Ahmed, Melting heat transfer in squeezing flow of basefluid (water), nanofluid (CNTs + water) and hybrid nanofluid (CNTs + CuO + water), *J. Therm. Anal. Calorim.* 143 (2021) 1157–1174.
- T. Hayata, Momani S. Inayatullah, K. Muhammad, FDM analysis for nonlinear mixed convective nanofluid flow with entropy generation, *Int. Commun. Heat Mass Transf.* 126 (2021), 105389.
- M. Arif, P. Kumam, W. Kumam, Z. Mostafa, Heat transfer analysis of radiator using different shaped nanoparticles water-based ternary hybrid nanomaterial with applications: a fractional model, *Case Stud. Therm. Eng.* 31 (2022), 101837.
- R.R. Sahoo, V. Kumar, Development of a new correlation to determine the viscosity of ternary hybrid nanomaterial, *Int. Commun. Heat Mass Transf.* 111 (2020), 104451.
- Z. Xuan, Y. Zhai, M. Ma, Y. Li, H. Wang, Thermo-economic performance and sensitivity analysis of ternary hybrid nanomaterials, *J. Mol. Liq.* 323 (2022) 114889.
- W. Ahmed, S.N. Kazi, Z.Z. Chowdhury, M.R.B. Johan, S. Mehmood, M.E. M. Soudagar, M.S. Ahmad, Heat transfer growth of sonochemically synthesized novel mixed metal oxide ZnO + Al<sub>2</sub>O<sub>3</sub> + TiO<sub>2</sub>/DW based ternary hybrid nanomaterials in a square flow conduit, *Renew. Sust. Energ. Rev.* 145 (2021), 111025.
- H. Adun, D. Kavaz, I. Wole-Osho, M. Dagbasi, Synthesis of Fe<sub>3</sub>O<sub>4</sub>-Al<sub>2</sub>O<sub>3</sub>-ZnO/water ternary hybrid nanomaterial: investigating the effects of temperature, volume concentration and mixture ratio on specific heat capacity, and development of hybrid machine learning for prediction, *J. Energy Stor.* 41 (2021), 102947.

- [30] S. Kashyap, J. Sarkar, A. Kumar, Performance enhancement of regenerative evaporative cooler by surface alterations and using ternary hybrid nanomaterials, *Energy* 225 (2021), 120199.
- [31] V. Kumar, R.R. Sahoo, Performance analysis of air heat exchanger equipped with various twisted turbulator inserts utilizing ternary hybrid nanomaterials, *Alexandr. Eng. J.* 61 (7) (2022) 5033–5050.
- [32] R.S.R. Gorla, I. Sidawi, Free convection on a vertical stretching surface with suction and blowing, *Appl. Sci. Res.* 52 (1994) 247–257.
- [33] M. Goyal, R. Bhargava, Boundary layer flow and heat transfer of viscoelastic nanofluids past a stretching sheet with partial slip conditions, *Appl. Nanosci.* 4 (2014) 761–767.
- [34] T. Gul, A. Saeed, Nonlinear mixed convection couple stress tri-hybrid nanofluids flow in a Darcy–Forchheimer porous medium over a nonlinear stretching surface, *Waves Random Complex Media* (2022) 1–18.
- [35] M.G. Reddy, N. Kumar, B.C. Prasannakumara, N.G. Rudraswamy, K.G. Kumar, Magnetohydrodynamic flow and heat transfer of a hybrid nanofluid over a rotating disk by considering Arrhenius energy, *Commun. Theor. Phys.* 73 (4) (2021), 045002.
- [36] B. Souayah, K.G. Kumar, M.G. Reddy, S. Rani, N. Hdhiri, H. Alfannakh, Slip flow and radiative heat transfer behavior of titanium alloy and ferromagnetic nanoparticles along with suspension of dusty fluid, *J. Mol. Liq.* 290 (2019), 111223.